Thin-Walled Structures 80 (2014) 159–166

Contents lists available at ScienceDirect

Thin-Walled Structures

journal homepage: www.elsevier.com/locate/tws

Experimental behaviour of cold-formed steel welded tube filled with concrete made of crushed crystallized slag subjected to eccentric load

Noureddine Ferhoune

Doctorate at Civil Engineering, University Larbi Ben Mhidi Oum El Bouaghi, Algeria

ARTICLE INFO

Article history:
Received 28 September 2013
Received in revised form
26 December 2013
Accepted 15 February 2014
Available online 12 April 2014

Keywords:
Composite columns
Concrete
Cold-formed
Strength
Rectangular hollow sections
Structural design

ABSTRACT

This paper presents results of tests conducted on thin welded rectangular steel stubs filled with concrete that gravel was substituted by 10 mm crushed crystallized slag stone. The studied section was made of two cold steel plates with U shape and welded with electric arc to form a steel box section. The cross-section dimensions were: $100 \times 70 \times 2$ mm^3. the main studied parameters were the stub height (200, 300, 400, 500 mm), the effect of the in filled concrete, the continued weld and the eccentric force. The tests were carried out 28 days after the date of casting. A total of 20 stubs were tested in a 50 tf machine up to failure, 4 stubs subjected to axial load compression and 16 stubs subjected to eccentric load compression along the minor and major rigidity axis. The aim of the study is to provide some evidences that the use of crushed slag could be integrated in the manufacturing of non-conventional concrete. All failure loads were predicted by using the Euro code 4 and the design method proposed by Z. Vrcelj and B. Uy. From test results, it was confirmed that the length of stubs and the eccentric load had a drastic effect on the load carrying capacity. The failure mode of composite stubs was a local buckling mode with all steel sides deformed outwards. The Euro code 4 loads predictions were generally in good agreement compared with experimental loads and on safe side. The loads results of design method proposed by Vrcelj and B. Uy were generally on safe side compared with experimental load except the columns subject to eccentric load with 400 mm and 500 mm height.

1. Introduction

Hollow structural steel sections are often filled with concrete to form a composite column. Traditional concrete-filled steel columns employ the use of hot rolled steel sections filled with concrete. These columns have been used wide spread as they speed up construction by eliminating formwork and producing high load carrying capacity. This leads to use small steel wall thickness and thus more economy. However, the major difficulty encountered is the local buckling of the steel wall especially in the case of stocky columns. Very few experiments have been undertaken on built up thin cold formed and welded steel sections filled with concrete or recycled materials such as slag gravel concrete. Tests of concrete-filled carbon steel tube columns were conducted by Schneider [1], Uy [2,3], Huang et al. [4], Han and Yao [5], Mursi and Uy [6], and many other researchers. Hollow structural steel sections are often filled with concrete to form a composite column. Traditional concrete filled steel columns employ the use of hot rolled steel sections filled with concrete. These columns have been used wide spread as they speed up construction by eliminating formwork and producing high load carrying [7]. This leads to use small steel wall thickness and thus more economy. However, the major difficulty encountered is the local buckling of the steel wall especially in the case of stocky columns [8]. Very few experimental is done on built up cold formed welded steel sections filled with concrete or recycled materials [9] such as slag stone concrete designated here by SSC. The latter has been tested under direct compression and was used as a filling material to overcome the undesired effects of imperfections of built up cold formed sections. The gain in strength was found to reach a value of up to 2 and decreased linearly with the stubs height [9]. No evidence is available in the literature to confirm the effect of using slag concrete and thin cold formed thin steel stubs on the behaviour and load carrying capacity. Also, the built up steel cross-section arrangements and welding nature are parameters that could have an effect on the strength of steel and composite stubs. The present work is a contribution to the understanding of the behaviour of short slag concrete filled cold formed thin steel stubs with different cross section and welding arrangements subjected to axial and eccentric load compression.

2. Expérimental programme

To study the behaviour of cold-formed steel welded tube filled with concrete made of crushed crystallized slag subjected to

E-mail address: noureddineferhoune@yahoo.fr

http://dx.doi.org/10.1016/j.tws.2014.02.014
0263-8231/

eccentric load, 20 steel tubes were prepared. All specimens had the cross section dimensions $100 \times 70 \times 2\ mm^3$. The main parameters studied were the stub height, the eccentric load and concrete core. Steel coupons were prepared to investigate the tensile yield steel strength. Six concrete cylinders were tested under direct compression at 28 days. 4 Composite stubs with different height were tested under axial compression, 8 composite tubes were tested under eccentric load along major axis rigidity (*xx*) axis and 8 along minor axis rigidity (*yy*) axis. The columns had end eccentricity ration in the range of 20–50%. The stub height varied from 200 mm to 500 mm. the slag stone concrete mix propriety are presented in Table 1 (Fig. 1).

2.1. Materials and fabrication

The concrete mix proportioning is presented in Table 1. The natural crushed stones were substituted by crushed crystallized slag of 10 mm size brought from iron manufacture ELHADJAR-ALGERIA. The use of such artificial stone instead of natural stone would contribute to environment protection by recycling such industrial waste. Steel coupons were prepared to investigate the tensile yield steel strength and concrete cylinders were tested under direct Compression after 28 days. The 28 days compression strength of SSC was 20 MPa. Young's modulus of concrete at 28 days was 21 GPa. The steel yield strength was 270 MPa with a Young's modulus of 205 GPa. The concrete core was vibrated externally by a shaking table for 2–3 min. All composite specimens were lefts in the curing room for a period of 28 days. Both, top and bottom faces of composite stubs were mechanically treated to remove surface irregularities and ensure that both steel and concrete are loaded during test. Al measured dimensions, material proprieties and the values of eccentricity are presented in Table 2.

2.2. Test rig and procedure

All specimens were tested in a 500 kN compressive machine, Figs. 2 and 3. Special attention was given to verifying the correct position of the stubs before any loading. For the first load increment, a complete check of strains and load was carried out. The load was applied on the composite section (concrete and steel), the top metal plate is the fixed plate (al degree of freedom were restrained except rotation belong *X* and *Y* axis), and the bottom metal plate is the moving plate (al degree of freedom were restrained, except rotation belong *X* and *Y* axis and displacement at load direction "belong *Z* axis") as shown in Fig. 2.

The specimen P1C, P2C, P3C and P4C had two strain gages, one in the vertical position and the second in the horizontal position at the opposite side to record vertical and horizontal steel strains ε_v and ε_h respectively. The other specimens subject to the eccentric load had only one strain gage in the vertical position Fig. 4. All strain gages were placed at mid-length section. During tests, graphical monitoring of load–strain relationships was carried out

Table 1
Slag stone concrete mix properties.

Cement content	**350 kg/m³**
Water–cement ratio	0.50
Aggregate-Sand	2.0
10 cm crushed slag stones	700 kg/m³
Sand	400 kg/m³
Slump	70 mm
Compressive strength at 28 days	20 MPa
Ec	21 GPa

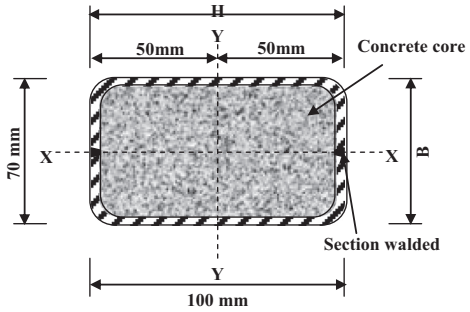

Fig. 1. Thin cold formed and welded steel cross section details.

Table 2
Measured dimensions and material properties.

Stubs no.	*B* (mm)	*H* (mm)	*t* (mm)	*L* (mm)	Eccentricity belong (*XX*) axis "*EX*" (mm)	Eccentricity belong (*YY*) axis "*Ey*" (mm)	f_y (MPa)	σ_{b28} (Mpa)
P1C	70	100	2.1	200	0	0	270	20
P1EX1	70	99	2	200	19.8	0	270	20
P1EX2	69	98	2.1	200	49	0	270	20
P1EY1	70	100	2	200	0	14	270	20
P1EY2	69	99	2	200	0	34.5	270	20
P2C	71	100	2	300	0	0	270	20
P2EX1	68	103	2	300	20.6	0	270	20
P2EX2	71	98	2	300	49	0	270	20
P2EY1	72	98	2	300	0	14.4	270	20
P2EY2	68	101	2	300	0	34	270	20
P3C	70	99	2	400	0	0	270	20
P3EX1	69	98	2.2	400	19.6	0	270	20
P3EX2	69	100	2	400	50	0	270	20
P3EY1	68	100	2.1	400	0	13.6	270	20
P3EY2	68	98	2.1	400	0	34	270	20
P4C	68	100	2.1	500	0	0	270	20
P4EX1	68	101	2	500	20.2	0	270	20
P4EX2	69	99	2.1	500	49.5	0	270	20
P4EY1	70	99	2.1	500	0	14	270	20
P4EY2	69	101	2	500	0	34.5	270	20

Fig. 2. View of test rig and sample P1EX1 after test.

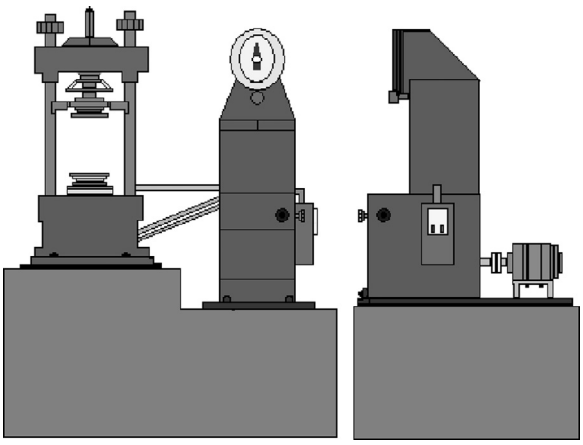

Fig. 3. Compressive machine.

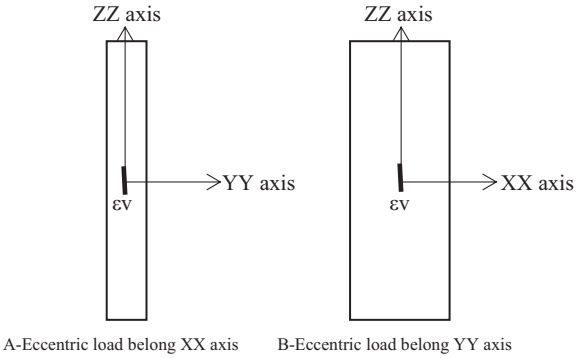

Fig. 4. Position of strain gage in the case of eccentric load.

to guide the running of experiment. The loading was performed up to failure. All data test results are gathered in Table 3.

3. Strength design codes

Euro code 4 (or EC4) is the most recently completed international standard in composite construction. EC4 provided a simplified method of design for composite columns, which was based on the European buckling curves for the influence of instability and on cross section interaction curves determining the column section's resistance. EC4 covers concrete encased and partially encased steel sections and concrete-filled sections with or without reinforcement. Design procedure of the composite columns considers the second-order effects including imperfections and ensures that under the most unfavourable combinations of actions at the ultimate limit state, instability does not occur [5]. The plastic resistance to compression $N_{pl.Rd}$ of a composite cross-section was calculated by adding the plastic resistance of its components:

$$N_{pl.Rd} = A_a f_y/\gamma_{Ma} + A_c(0.85 f_{ck}/\gamma_c) + A_s f_{sk}/\gamma_s \quad (1)$$

where A_a, A_c and A_s are the cross-sectional areas of structural steel, concrete and reinforcement respectively; f_y, f_{ck} and f_{sk} are respectively the yield stress of steel cross section, the strengths of concrete and the yield stress of steel reinforcement; γ_{Ma}, γ_c and γ_s are partial safety factors at the ultimate limit states.

According EC3 the load carrying capacity for steel columns section is calculated by formula (2).

$$N_{b.Rd} = \chi\beta_A A_a f_y/\gamma_{Ma} \quad (2)$$

where $\beta_A = 1$ for classes Sections 1–3, and $\beta_A = A_{effectif}/A$ for class Section 4, χ is a reduction coefficient of load carrying capacity in order to take into account the phenomenon of buckling [4].

3.1. Resistance to combined compression and bending

It is necessary to satisfy the resistance requirements in each of the principal planes, taking account of the slenderness, the bending moment diagram and the bending resistance in the plane under consideration. The cross-sectional resistance of a composite column under axial compression and uniaxial bending is given by an interaction curve as shown in Fig. 4.

The point D on this interaction curve corresponds to the maximum moment resistance M_{max}, Rd that can be achieved by the section. This is greater than $M_{pl.Rd}$ because the compressive axial force inhibits tensile cracking of the concrete, thus enhancing its flexural resistance. The above interaction curve can be determined point by point, by considering different plastic neutral axis positions in the principal plane under consideration. The concurrent values of moment and axial resistance are then found from the stress blocks, together with the two equilibrium equations for moments and axial forces (Fig. 5).

Point A: Axial compression resistance alone

$$N_A = N_{pl.Rd} \quad M_A = 0 \quad (3)$$

Point B: Uniaxial bending resistance alone

$$N_B = 0 \quad M_B = M_{pl.Rd} \quad (4)$$

Here it can be seen, that in the determination of the resistance of the cross-section, concrete regions in tension are taken as being cracked and ineffective.

Point C: Uniaxial bending resistance identical to that at point B, but with non-zero resultant axial compression force:

$$N_C = N_{pm.Rd} = A_{C.fcd} \quad M_C = M_{pl.Rd} \quad (5)$$

Point *D*: Maximum moment resistance

$$N_D = 0.5\, A_C f_{cd}$$
$$M_D = M_{max\ .Rd} = (W_{pa} f_{yd}) + (W_{ps} f_{sd}) + (0.5 W_{pc} f_{cd}) \quad (6)$$

W_{pa}, W_{ps}, and W_{pc} are the plastic modular respectively of the steel section, the reinforcement and the concrete.

Point E: Situated midway between A and C.

The enhancement of the resistance at point E is little more than that given by direct linear interpolation between A and C, and the calculation can therefore be omitted. It is usual to substitute the linearised version AECDB (or the simpler ACDB) shown in Fig. 4 for the more exact interaction curve, after doing the calculation to determine these points.

4. Design method proposed by Vrcelj and Uy [10]

Vrcelj and Uy [10] proposed a design method for the strength calculation of a slender concrete filled steel box column loaded in compression, when the steel portion of the composite column is affected by local buckling. The following relationship is proposed by Vrcelj and Uy [10]:

$$N_{clb} = \alpha_{1b} N_c \quad (7)$$

where N_{clb} is the slender column buckling load which incorporates local buckling, N_c is the column buckling load and α_{1b} is the interaction coefficient to account for local buckling and is in the

Table 3
Results of concrete filled steel stubs.

Stubs no.	Eccentricity belong (*XX*) axis eX (mm)	Eccentricity belong (*YY*) axis ey (mm)	Experimental load (kN) (*P* test)	EC 4 load (kN) (P EC4)	Load design method of Z. Vrcelj and B. Uy (P Vrcelj)	P EC4/*P* test	*P* Vrcelj/*P* test
P1C	0	0	290	269.8	276.3	0.93	0.95
P1EX1	19.8	0	278.1	260.5	267.1	0.93	0.96
P1EX2	49	0	263.3	257.9	269.4	0.97	1.02
P1EY1	0	14	272.6	262.6	269.2	0.96	0.98
P1EY2	0	34.5	260.9	257.9	264.5	0.98	1.01
P2C	0	0	270	263.6	271.9	0.97	1.01
P2EX1	20.6	0	263.1	259.2	270.2	0.98	1.02
P2EX2	49	0	251.9	251	267.6	0.99	1.06
P2EY1	0	14.4	253.4	250.5	270.2	0.98	1.06
P2EY2	0	34	248.2	249.7	266	1.01	1.07
P3C	0	0	265	252	267.1	0.95	1.0
P3EX1	19.6	0	251	248	276.4	0.98	1.1
P3EX2	50	0	237	235.9	266.6	0.99	1.12
P3EY1	0	13.6	248.5	240.4	271	0.96	1.09
P3EY2	0	34	232.5	233.8	266.7	0.98	1.14
P4C	0	0	262.3	241.7	271	0.92	1.03
P4EX1	20.2	0	243	237	266	0.97	1.09
P4EX2	49.5	0	235	226.3	271.5	0.96	1.15
P4EY1	0	14	238	224.5	274.2	0.94	1.15
P4EY2	0	34.5	232	223.4	268.7	0.96	1.15

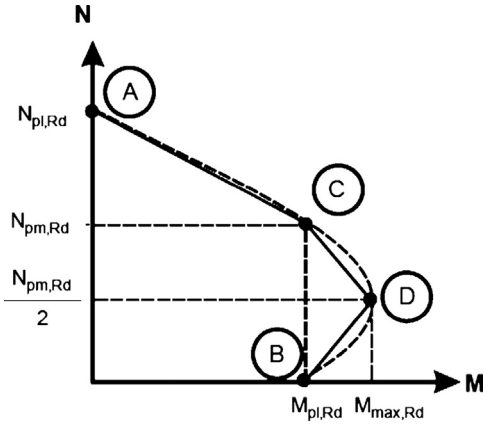

Fig. 5. Interaction curve with linear approximation.

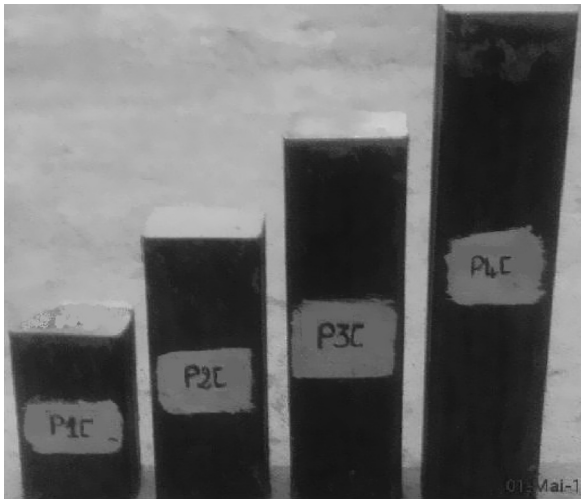

Fig. 6. Columns subject to axial compression.

range $0 \leq \alpha 1b \leq 1.0$.

α_{1b} is calculated as : $\alpha_{1b} = (100 - \rho_r)/100$ (8)

where the percentage reduction, ρ_r is given as:

$\rho_r = [(N_c - N_{clb})/N_c] \times 100$ (9)

5. Results of stub tests

The results of the tests carried out on cold-formed steel welded tubes filled with concrete made of crushed crystallized slag are discussed here, and is followed by a comparison between the experimental results and the theoretical Eurocode4 prediction. A total of 20 rectangular stubs were tested in compression. The main parameters studied were the stub height, the effect of the in filled concrete, the continued weld and the eccentric force. Details of test specimens including are given in Table 2. The test programme included 3 groups of specimens. The first group gathered the tubes tested to axial compression (P1C, P2C, P3C and P4C) Fig. 6, the second group shown in Fig. 7 was the stubs tested to eccentric load compression according to (*xx*) axis (P1EX1, P1EX2, P2EX1, P2EX2, P3EX1, P3EX2, P4EX1 and P4EX2) and the third group shown in Fig. 8 included composite stubs that were tested at eccentric load compression along (*yy*) axis (P1EY1, P1EY2, P2EY1, P2EY2, P3EY1, P3EY2, P4EY1 and P4EY2). The percentage of eccentricity load is 20% and 50% according to major and minor rigidity axis.

All eccentric and concentric columns showed sign of local buckling as loading continued except column P4EX2 and P4EY2, the mode of instability of this two columns is a local buckling governed by the global buckling with the development of plastic hinge at the region of local buckling. The load increased with the increase of deformations. The deformation induced a moment due to load–displacement effect. The column failed when the local buckling created a plastic hinge that exhausted the strength of the column section.

The results obtained from testing the first group at axial compression show that the main feature of this composite tube is the local buckling that took place in all samples with a small attenuation for longer steel stubs. Both, large and small sides buckled outwards. The decrease in the composite tube load carrying capacity with the stub height increase is well pictured in Fig. 9. The load carrying capacity varied from 262.3 kN to 290 kN and the maximum strain registered in this group is 2661.13 micro-strains Fig. 10.

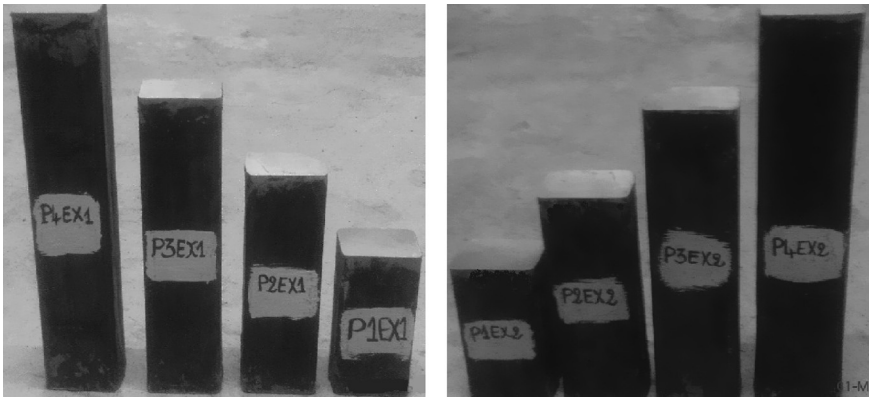

Fig. 7. Columns subject to eccentric load according (*xx*) axis.

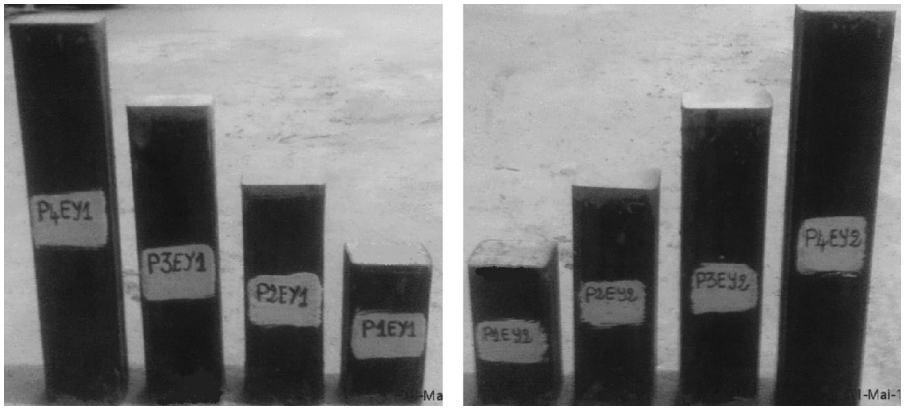

Fig. 8. Columns subject to eccentric load according (*yy*) axis.

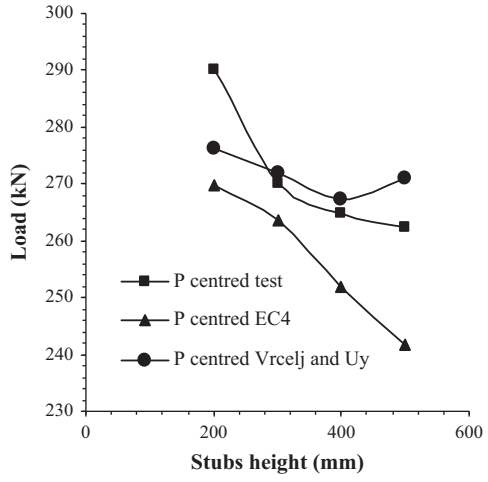

Fig. 9. Experimental, EC4 and Vrcelj design method failure loads for first group.

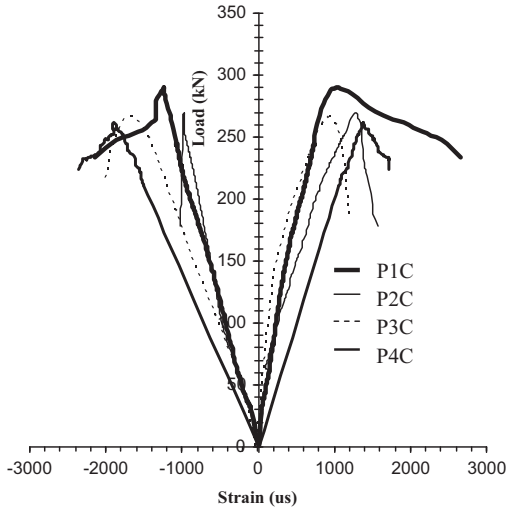

Fig. 10. Load–strain curve of first group.

The test results of the second group subject to eccentric load along (*xx*) axis confirm the diminution of load carrying capacity when the eccentricity according (*xx*) axis increases. The small sides of the composite section in this case buckled outwards significantly compared with large side Figs. 2 and 11. The load carrying capacity varied from 235 kN to 178.1 kN and the maximum strain registered is 3513.14 micro-strains. All loads–strain curve of this group are presented in Figs. 13–16.

The last group was tested under eccentric load along (*yy*) axis. Results obtained from testing the third group are presented in Table 3 and the load–strain curve are presented in Figs. 13–16. The load carrying capacity is influenced by the augmentation of eccentricity according (*yy*), we see that the load decreases significantly, compared with previous group, when the eccentricity along minor axis (*yy*) increases. The mode of instability in this case is a local buckling, contrary to the preceding group, the large side buckled outwards significantly compared with small side (Fig. 12). The maximum value of strain registered in this case is 3874.19 micro-strains.

Load–strain relationships obtained from testing the three groups of columns are shown in Figs. 10 and 13–16. The main feature of these curves is the linear ascending branch up to failure followed by a softening descending branch. A significant decrease

Fig. 11. P2EX2 and P4EX2 columns after test.

Fig. 12. P2EY1 and P2EY2 columns after test.

in the failure load and stiffness are recorded when the eccentricity increase especially when the eccentricity is along (*yy*) axis.

6. Discussion

The experimental results shown that the cold-formed steel welded tube filled with concrete made of crushed crystallized slag can be used in structure of building. The default of cold-formed steel welded tube is partially eliminated by concrete core. The mode of instability in the case of this columns tested is the local buckling except column P4EX2 and P4EY2, the mode of instability of this two columns is a local buckling governed by the global buckling. Results shown that the load carrying capacity is sensitive to: column height, the eccentricity and his direction.

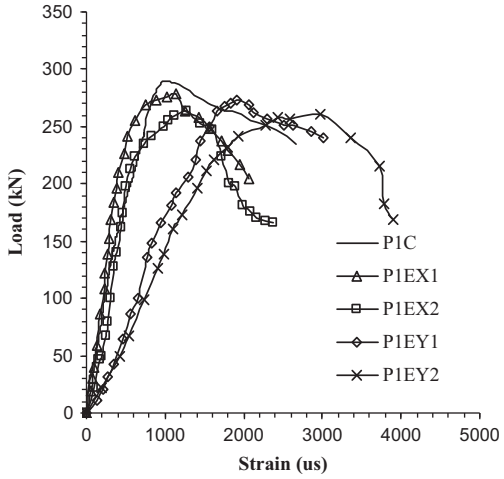

Fig. 13. Load–strain curve of P1C, P1EX1, P1EX2, P1EY1 and P1EY2 columns.

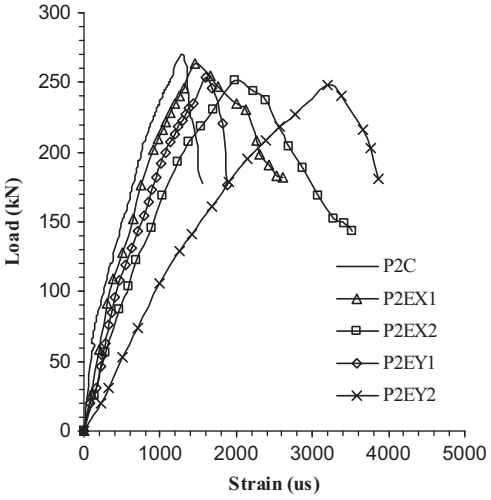

Fig. 14. Load–strain curve of P2C, P2EX1, P2EX2, P2EY1 and P2EY2 columns.

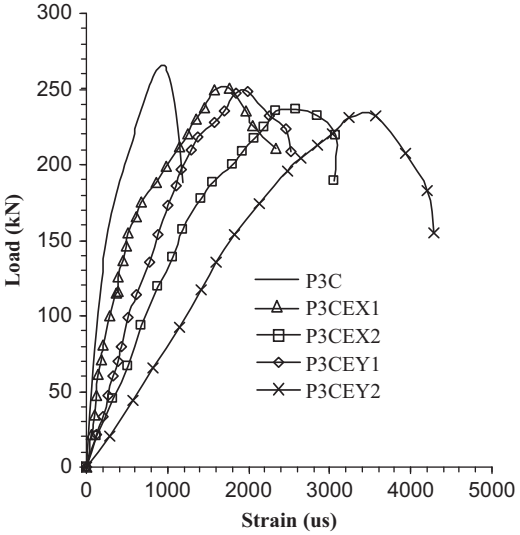

Fig. 15. Load–strain curve of P3C, P3EX1, P3EX2, P3EY1 and P3EY2 columns.

Figs. 17 and 18 presents the variation of load carrying capacity with stubs height; we see that the axial or eccentric load increase when the stubs height decreases, the relationship between load

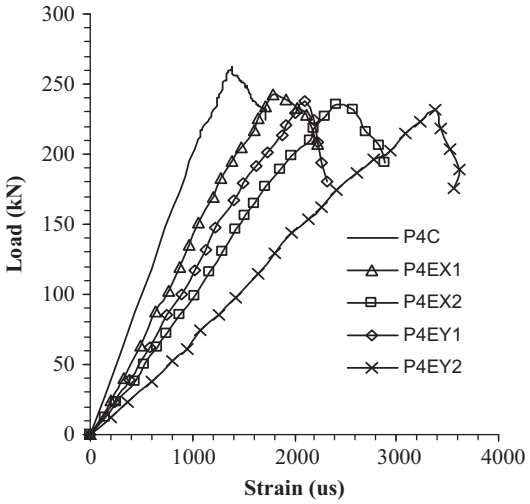

Fig. 16. Load–strain curve of P4C, P4EX1, P4EX2, P4EY1 and P4EY2 columns.

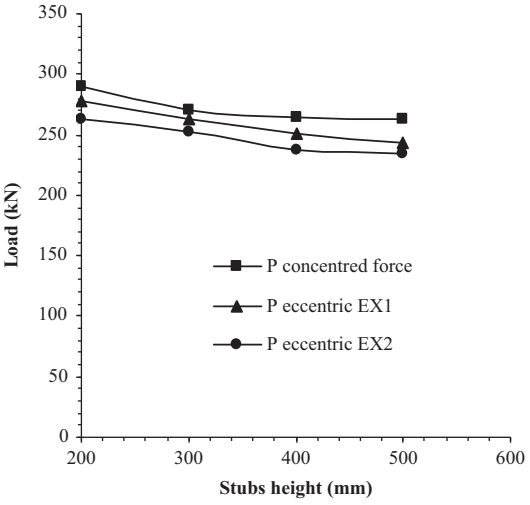

Fig. 17. Load–stubs height relationship of columns subject to eccentric load along (*xx*) axis.

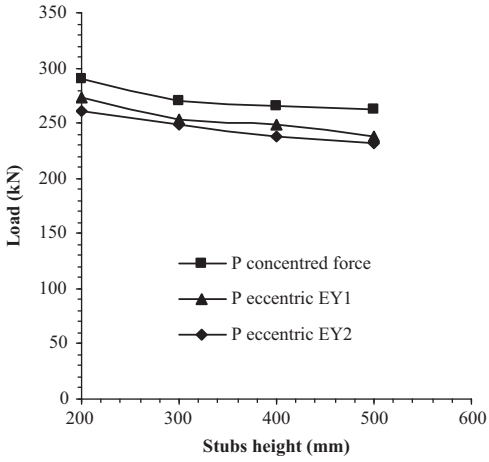

Fig. 18. Load–stubs height relationship of columns subject to eccentric load along (*yy*) axis.

and stubs height is almost linear. The rate of decrease load when stubs height increase varied from 6.8% to 9.6% for columns subject to concerted force, from 5.3% to 10.8% for stubs subject to eccentric load along (*xx*) axis and from 7% to 11.1% in the case of columns subject to eccentric load along (*yy*) axis.

Figs. 19 and 20 exposed the effect of eccentricity on the load carrying capacity of cold-formed steel welded tube filled with concrete made of crushed crystallized slag. It is clear to see that the load carrying capacity decreases when the eccentricity along minor or major rigidity axis increases. The percentage of diminution of load carrying capacity of stubs subject to eccentric load compared to stubs subject to axial load varied from 6.7% to 10.5% in the case of stubs subject to eccentric load along (*xx*) axis and from 8% to 11.5% in the case of stubs subject to eccentric load according (*yy*) axis.

Table 3 shows the Eurocode4 theoretical prediction and the results of design method proposed by Vrcelj and Uy [10] of composite stubs tested in this study. The load predicted by EC4 of stubs subject to concentred force varied from 241.7 kN to 269.8 kN and from 267.2 kN to 276.4 kN in the case of simplify method proposed by Z. Vrcelj and B. Uy. For the columns subject to eccentric load according (*xx*) axis, the EC4 load varied from 226.3 kN to 260.5 kN and the load simplify method varied from 266 kN to 276.4 kN. In the case of stubs subject to eccentric load along (*yy*) axis, the EC4 load prediction varied from 223.4 kN to 262.6 kN, and the load simplify method proposed by Z. Vrcelj and B. Uy varied from 266 kN to 274.2 kN.

Generally, results of load carrying capacity obtained by EC4 were in good agreement with experimental load and on safe side. The error of under estimate of load carrying capacity using EC4

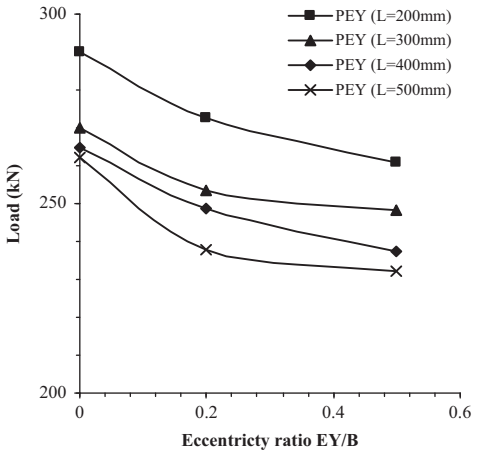

Fig. 19. Load–eccentricity ratio (*EX*/*H*) relationship of columns.

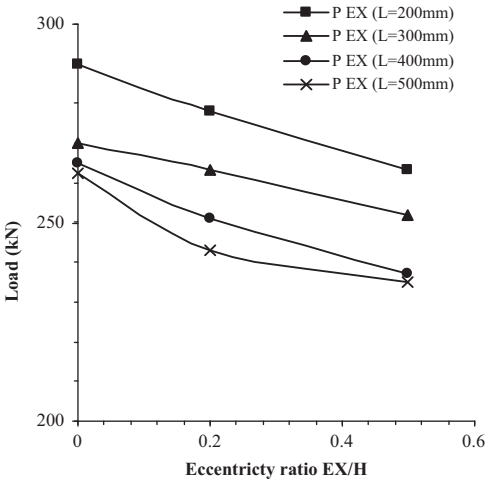

Fig. 20. Load–eccentricity ratio (*EY*/*H*) relationship of columns.

Table 4
Summary of test observations.

Stubs no.	Load at start of first buckling (kN)	Distance from top to first local buckle (mm)	Experimental load (kN)
P1C	275.8	38.3	290
P1EX1	253.6	76.6	278.1
P1EX2	230.7	103.3	263.3
P1EY1	250.8	54.7	272.6
P1EY2	216.5	66.8	260.9
P2C	253.9	51.4	270.
P2EX1	243.4	114.7	263.1
P2EX2	220.7	265.7	251.9
P2EY1	218.4	194.4	253.4
P2EY2	206.1	132.2	248.2
P3C	246.5	96.5	265
P3EX1	228.9	203.2	251
P3EX2	204.2	194.8	237
P3EY1	217.8	285.4	248.5
P3EY2	197.3	302.2	232.5
P4C	238.5	284.6	262.3
P4EX1	203.1	112.4	243
P4EX2	195.4	96.7	235
P4EY1	198.2	201.5	238
P4EY2	177.3	187.8	232

prediction varied from 0.47% to 6.9%. The loads results of design method proposed by Vrcelj and B. Uy were generally in good agreement and on safe side compared with experimental loads except the columns subject to eccentric force with 400 mm and 500 mm height, thus in this case the load design method is on unsafe side. The error of estimation of load using method proposed by Vrcelj and B. Uy varied from 0.7% to 15.8%.

The load at start of first buckling and distance from top to first local buckle are indicated in Table 4. The load at start of first buckling registered varied from 177.3 kN to 275.8 Kn. The minimum distance from top to first local buckle registered is 38.3 mm in the case of column P1C and the maximum value registered is 302.2 mm for stub P3EY2.

7. Conclusion

In this study we have presented results of tests conducted on thin welded rectangular steel stubs filled with concrete that gravel was substituted by 10 mm crushed crystallized slag stone. The behaviour of eccentrically loaded of these columns highlighting the performance of concrete core made of crushed crystallized slag compared with normal concrete. The capacity of the columns is based upon the increased strength of confined concrete and the increased steel plate buckling capacity due to composite action. The column strengths test were compared with the design strengths calculated using the European code EC4, it is shown that the design strengths calculated using the European code are in good prediction and on safer side, but the design method proposed by Vrcelj and B. Uy is on unsafe side in the case of columns with length 400 mm and 500 mm subject to eccentric load. In conclusion, the performance of crushed crystallized slag stone in composite columns is found satisfactory and in future the crushed crystallized slag can be used as a potential source of alternative aggregate. The using of crushed crystallized slag as an aggregate in the composition of concrete core participates at the environmental protection.

References

[1] Schneider SP. Axially loaded concrete-filled steel tubes. J. Struct. Eng., ASCE 1998;124(10):1125–38.
[2] Uy B. Local and post-local buckling of concrete filled steel welded box columns. J. Constr Steel Res. 1998;74(1–2):47–72.
[3] Uy B. Static long-term effects in short concrete-filled steel box columns under sustained loading. ACI Struct J 2001;98(1):96–104.
[4] Huang CS, Yeh YK, Hu HT, Tsai KC, Weng YT, Wang SH, et al. Axial load behavior of stiffened concrete-filled steel columns. J Struct Eng, ASCE 2002;128(9):1222–30.
[5] Han LH, Yao GH. Influence of concrete compaction on the strength of concrete-filled steel RHS columns. J Constr Steel Res 2003;59(6):751–67.
[6] Mursi M, Uy B. Strength of concrete filled steel box columns incorporating interaction buckling. J Struct Eng, ASCE 2003;129(5):626–39.
[7] Zeghiche J. 'Concrete filled steel tubes' [Ph.D. thesis]. University of Annaba; 2005.
[8] Bassam Z, Emhaidy SG. Enhancing filled-tube properties by using fiber polymers in filling matrix. J Appl Sci 2005;5(2):232–5.
[9] Yang You-Fu, Han Lin-Hai. Experimental behaviour of recycled aggregate concrete filled steel tubular columns. J Constr Steel Res 2006;62(12):1310–24.
[10] Vrcelj Z, Uy B. Strength of slender concrete-filled steel box columns incorporating local buckling. J Constr Steel Res 2002;58(2):275–300.